

The role of NLRC4 inflammasome on intracerebral hemorrhage-caused inflammation in rats

Hui Gan

Chongqing Medical University

Li Zhang

Chongqing Medical University

Hui Chen

Chongqing Medical University

Han Xiao

Chongqing Medical University

Lu Wang

Chongqing Medical University

Xuan Zhai

Chongqing Medical University Affiliated Children's Hospital

Ning Jiang

Chongqing Medical University

Ping Liang (✉ liangping868@sina.com)

Chongqing Medical University Affiliated Children's Hospital

Jing Zhao

Chongqing Medical University

Research

Keywords: NLRC4 inflammasome, LRRK2, RGS2, Intracerebral hemorrhage, inflammation

Posted Date: August 4th, 2020

DOI: <https://doi.org/10.21203/rs.3.rs-44218/v1>

License: © ⓘ This work is licensed under a Creative Commons Attribution 4.0 International License.

[Read Full License](#)

The role of NLRC4 inflammasome on intracerebral hemorrhage-caused inflammation in rats

Hui Gan,^{1,2,3,4} Li Zhang,^{1,2} Hui Chen,^{1,2} Han Xiao,^{1,2} Lu Wang,^{1,2} Xuan Zhai,^{1,2} Jiang Ning,^{3,4} Ping Liang^{1,2,*} and Jing Zhao,^{3,4,*}

1 Department of Neurosurgery; Ministry of Education Key Laboratory of Child Development and Disorders; National Clinical Research Center for Child Health and Disorders; China International Science and Technology Cooperation base of Child development and Critical Disorders; Children's Hospital of Chongqing Medical University, Chongqing, P.R China, Chongqing 400010, China

2 Chongqing Key Laboratory of Translational Medical Research in Cognitive Development and Learning and Memory Disorders, Chongqing 400010, China

3 Department of Pathophysiology, Chongqing Medical University, Chongqing 400010, China

4 Institute of Neuroscience, Chongqing Medical University, Chongqing 400010, China

*Correspondence: zhaojing@cqmu.edu.cn(J.Z.);liangping868@sina.com(P.L.);Tel./Fax: (+86)23-6362-8729

Author details:

Name	Institute	Email Address
Hui Gan	Chongqing Medical University	191353055@qq.com
Li Zhang	Chongqing Medical University	1353753933@qq.com
Hui Chen	Chongqing Medical University	chenhuimed@sina.com
Han Xiao	Chongqing Medical University	373160654@qq.com
Lu Wang	Chongqing Medical University	1373771266@qq.com
Xuan Zhai	Children's Hospital of Chongqing Medical University	zhaixuan@163.com
Jiang Ning	Chongqing Medical University	308473169@qq.com
Ping Liang	Children's Hospital of Chongqing Medical University	liangping868@sina.com
Jing Zhao	Chongqing Medical University	zhaojing@cqmu.edu.cn

Abstract:

Background: The NLRC4 inflammasome, a member of nucleotide-binding and oligomerization domain-like receptor (NLR) family, amplifies the neuroinflammation by facilitating the processing of caspase-1, interleukin (IL)-1 β and IL-18. We explored whether NLRC4 knockdown alleviated inflammatory injury following intracerebral hemorrhage (ICH). Furthermore, whether NLRC4 inflammasome activation can be adjusted by the RGS2/LRRK2 pathway was investigated.

Methods: 50 μ l arterial blood was drawn and injected into basal ganglia to simulate the ICH model. NLRC4 small interfering RNAs (siRNA) were utilized to knockdown NLRC4. LRRK2 inhibitor (GNE7915) was injected into the abdominal cavity. Short hairpin (sh) RNA lentiviral and lentivirus containing RGS2 were designed and applied to knockdown and promote RGS2 expression. Neurological functions, brain edema, western blot, enzyme-linked

immunosorbent, hematoxylin and eosin staining, nissl staining, immunoprecipitation, immunofluorescence assay and evans blue dye extravasation and autofluorescence assay were evaluated.

Results: It was shown that the NLRC4 inflammasome was activated following ICH injury. NLRC4 knockdown extenuated neuronal death, damage of the blood-brain barrier, brain edema and neurological deficiency at 3 d after ICH. NLRC4 knockdown reduced myeloperoxidase (MPO) cells as well as IL-1 β and IL-18 following ICH. GNE7915 reduced LRRK2 kinase, the combination of LRRK2 and NLRC4 and NLRC4 inflammasome activation. RGS2 suppressed the combination of LRRK2 and NLRC4, and NLRC4 inflammasome activation through regulating LRRK2 Kinase Activity.

Conclusion: Our study demonstrated that the NLRC4 inflammasome may aggravate the inflammatory injury induced by ICH and RGS2/LRRK2 may relieve inflammatory injury by restraining the NLRC4 inflammasome activation.

Keyword: NLRC4 inflammasome, LRRK2, RGS2, Intracerebral hemorrhage, inflammation

1. Background

Intracerebral hemorrhage (ICH) is featured by high mortality and high disability¹, although it accounts for 10–15% of all stroke types². However, there is currently no effective therapy for ICH³. Much evidence has shown that intracerebral hemorrhage leads to a series of pathophysiological changes including inflammation, edema, apoptosis and necrosis⁴. Inflammation has been regarded as a key role in ICH induced injury⁵ by releasing proinflammatory cytokines⁶, especially the interleukin (IL)-1 β ⁷. IL-18 also has been reported to contribute to neuronal injury and cell death⁸. Increased expressions of IL-1 β and IL-18 are often observed upon brain injury^{9,10}. Inflammasome, a part of the innate immune system, can cut pro-caspase-1 into cleaved caspase-1, which makes the pro-interleukin-1 β as well as the pro-interleukin-18 mature and causes inflammatory responses^{11,12}.

The nucleotide-binding and oligomerization domain-like receptor (NLR) family responds to innate immunity by forming inflammasomes^{13,14}. Different from many other NLR members, the NLRC4 (CARD12, IPAF) could recruit pro-caspase-1 directly through its CARDs without ASC, although ASC contributes to the maturation of IL-1 β , cleaved caspase-1 and IL-18^{12,15}. Moreover, the phosphorylation at NLRC4-Ser⁵³³ is critical in the activation of the NLRC4 inflammasome^{16,17}. The NLRC4 inflammasome is activated in bacterial inflammation^{18,19}. However, the neuroinflammation in several diseases, such as traumatic brain injury²⁰, ischemic stroke²¹, and ICH is a sterile inflammation. The phosphorylation at NLRC4-Ser⁵³³ and the activation of the NLRC4 inflammasome after ICH remain to be elucidated.

The multi-domain protein Leucine-rich Repeat Kinase-2 (LRRK2) consists of the GTPase domains, the functional kinase domains and multiple domains for protein-protein interaction²². LRRK2 has been well known as a kinase closely related to Parkinson's disease (PD)^{23,24}. Abnormally high LRRK2 kinase activity is related to neurotoxicity and some pathogenic LRRK2 mutations such as G2019S²⁵, I2020T²⁶ and R1441C/G/H²⁷. Intriguingly, Cui H and his colleagues have shown that LRRK2 kinase can activate the NLRC4 inflammasome in acute *Salmonella typhimurium* infection by promoting the phosphorylation of NLRC4 at

Ser533 with interaction with NLRC4²⁸. However, whether the role of NLRC4 in the inflammatory response is regulated by LRRK2 after ICH remains unclear.

The regulator of G protein signaling 2 (RGS2) consists of a single RGS domain with minimal flanking amino and carboxy-terminal regions, which has a length of 24 kDa²⁹. Our previous study has shown that the RGS2 expression was upregulated and relieved inflammatory injury in the collagenase-induced intracerebral hemorrhage model. The protective role of RGS2 in anxiety³⁰, panic disorder, and suicide³¹ has been reported. It has been indicated that RGS2 modulates LRRK2 function by restricting its kinase activities on a Parkinson's disease³².

Therefore, our study aimed to investigate whether the NLRC4 inflammasome is activated by the phosphorylation at NLRC4-Ser⁵³³ after ICH. We also explored whether LRRK2 aggravates the NLRC4 inflammasome and RGS2 regulates activation of the NLRC4 inflammasome after ICH via LRRK2 kinase.

2. Materials and Methods

Rats

Sprague-Dawley rats(healthy, male and adult) were purchased from Chongqing Medical University with the license of the institutional animal care and use committee. All the rats were housed under constant temperature (25-26°C) with sufficient food and water. All efforts were made to relieve pain and unintentional death^{5,33}.

ICH models

The rats first underwent intraperitoneal anesthesia with 4% of 1 ml/100g chloral hydrate. Then, 50uL of autologous blood was taken from the femoral artery by a microinjection pump (Shenzhen Ruiwode Life Technology Co., Ltd., China) on the operation side with a micro syringe washed by heparin. Afterwards, these rats were fixed on a stereotaxic apparatus (Shenzhen Ruiwode Life Technology Co., Ltd., China). The blood was automatically infused into their right basal ganglia within 5min at 3.00 mm from the midline, 0.2 mm behind the bregma, and 5.80 mm beneath the cortex. The needle was left for 10 min to prevent blood reflux before suturing the scalp. Throughout the experiment, the rats were put in thermostatic blankets to keep the body temperature at roughly 37°C. The sham group was only given a needle insertion.

siRNA Transfections

NLRC4-siRNA was centrifuged and dissolved in 12.5uL RNase-free water at a concentration of 2 µg/µL before being oscillated, centrifuged and infused and retained for 10 min into the right lateral ventricle at 1 mm anterior–posteriorly, 2 mm mediolaterally, and 3.5 mm dorsoventrally.^{34,35} The siRNA-NLRC4 and scramble siRNA (known as si-NC or si-negative control) were transfected at 36h after the ICH model establishment. Both were obtained from GenePharma (China): NLRC4-siRNA(sense: GCUGAGCCCCACGUAUAAATT; antisense: UUUUAUACGUGGGCCUCAGCTT); the scramble siRNA (sense:UUCUCCGAACGUGUCACGUTT; antisense:ACGUGACACGUUCGGAGAATT)

Inhibitor GNE7915 Injection

5% DMSO, 30% PEG 300, 5% Tween 80 and ddH₂O was added to the inhibitor GNE-7915 at a concentration of 3.1 mg/mL GNE7915 was intraperitoneally injected(50 mg/kg) into the rats at 60h after ICH³⁶.

Lentivirus Transfection

Rats were put in a stereotactic frame (Shenzhen Ruiwode Life Technology Co., Ltd., China) after being anesthetized using 4% C₂H₃Cl₃O₂. The lentivirus vectors (Lenti-RGS2) for RGS2 overexpression and the short hairpin (sh) RNA (sh-RGS2) for RGS2 knockdown were produced (GenePharma Technology Corporation, PRC): Lenti-RGS2(sense: TTCTCCGAACGTGTCACGT); sh-RGS2(sense: GCTCTGGGCAGAAGCATTGA). Holes were made in the rats' pericranium 1.9 mm behind the coronal suture and 0.9 mm from the sagittal suture. Then, a 10 μ L sized microinjection pump was put stereotactically 3.5 mm deeper under the cortex. 5 μ L of lentivirus with 1×10^9 genomic copies of Lenti-RGS2 and short hairpin (sh) RNA-RGS2 (sh-RGS2) were injected to the right lateral cerebral ventricle ipsilaterally at 0.5 μ L/min. 10 min after injection, the needle was slowly withdrawn. The rats were then taken back to heal ³⁷. Four weeks later, these 9-week-old rats underwent ICH surgery³⁸.

Brain water content

The brain-water content was assessed using the wet-dry method³⁹. Under deep anesthesia, ICH rats were decapitated at 72h after ICH, and the brain was quickly removed. The brain was divided into ipsilateral (hemorrhagic) side and contralateral side, weighed on an analytical microbalance and then dried under 100°C for 48h to determine the dry weight. The brain-water content (%) was measured accordingly (wet weight–dry weight)/wet weight \times 100%.

The modified Neurological Severity Score

Motor, sensory (visual, tactile, and proprioceptive), balance and reflex tests were included in the modified Neurological Severity Score⁴⁰. Neurological severity of the rats on day 3 after ICH was assessed by a score of 0 to 18, with 0 indicating normal score and 18 indicating maximum neurological deficit⁴¹.

Western blotting

After perfusion of normal saline from the heart, 4% paraformaldehyde was slowly infused to the whole body for internal fixation at 72h after ICH. The brains were removed and the proteins of peripheral hematoma were extracted by extraction reagents (Beyotime, China). Concentrations of the protein samples were calculated with an enhanced BCA Protein Assay Kit (Beyotime, PRC). Proteins were then loaded (50 μ g) and separated by 6%, 8% and 15% SDS-PAGE gel electrophoresis and then moved to polyvinylidene fluoride (PVDF, Millipore, USA). After blocking with 5% nonfat milk for 2h, they were incubated overnight at 4°C with the primary antibodies: rabbit anti-NLRC4 (1:800, Novus Biologicals, USA), mouse anti-pNLRC4 (1:400, ECM Biologicals, USA), mouse anti-RGS2 (1:500, Santa Cruz, USA), rabbit anti-cleaved caspase-1(1:500, Cell Signaling, USA), rabbit anti-cleaved IL-1 β (1:500, Affinity, USA), rabbit anti-cleaved IL-18 (1:200, R&D, USA), rabbit anti-LRRK2 (1:1000, Abcam, USA), rabbit anti-pLRRK2 s935(1:500, Abcam, USA)and rabbit anti- β -actin (1:1000, Proteintech, USA). On the next day, the fluorides were washed for 5 times (6 min/wash) in

TBST. The secondary antibody (1:2000, Proteintech, USA) linked horseradish peroxidase (HRP) was added on the bands for 2h. The ECL detection reagents (Thermo, USA) were used to visualize the bands. ImageJ software was used for the relative density of these proteins.

Hematoxylin and eosin (H&E) staining

After perfusion of normal saline from the heart, 4% paraformaldehyde was slowly infused to the whole body for internal fixation at 72h after ICH. The brains were removed, fixed with 4% paraformaldehyde for 48 h, and dehydrated using 75%, 80%, 95% and 100% alcohol. Then, the brains were transparentized, dipped in wax and cut into brain sections (5 μ m thick) by the slicer. After dewaxing, debenzene, hematoxylin staining and eosin staining, the brain sections were dehydrated, transparentized, and observed under a microscope.

Nissl staining

The brain sections were made using the above method. After being debenzened and deparaffinized, brain sections underwent staining in a tar purple solution for 15 min before being washed in ddH₂O. The brain sections went through color separation reaction, and were then dehydrated in 70%, 80%, 95% and 100% ethanol, respectively. Finally, the sections were transparentized, mounted and observed under the microscope (\times 400 magnification). Neurons in the area around the hematoma were counted per microscopic field.

Immunofluorescence staining

Consecutive coronal sections of the brain (8 μ m thick) were then blocked in 5% Bovine Serum Albumin (BSA) at 37°C for 1 h. They were incubated with rabbit anti-mouse MPO antibody (1:50, Abcam, USA), rabbit anti-mouse NLRC4 antibody (1:100; Novus Biologicals, USA) and mouse anti-mouse LRRK2 antibody (1:100; Milipore Biologicals, USA) overnight at 4°C. The samples were then incubated after three cycles of PBS washing with corresponding fluorescence-conjugated secondary antibodies (1:100; Proteintech, USA) for 1h at 37°C. Three cycles of PBS washing were again performed. Microphotographs were analyzed with Image J software, and Pearson's Coefficient was used to evaluate the combination of NLRC4 and LRRK2.

Evans Blue Dye Extravasation and Autofluorescence

At day 3 after ICH, Evans blue dye (4%, 5ml/kg, Sigma-Aldrich) was injected into the femoral vein under anesthesia. After 1 h, the rats were perfused with normal saline, and brain tissues were collected. 50% trichloroacetic acid was put onto the brain tissues around the hematoma before the sample was homogenized and centrifuged at 12,000 g for 30 min. The absorbance of the resulting supernatant was measured by a spectrophotometer at 620nm. Meanwhile, the brains were cut into 8 μ m slices and observed under a fluorescent microscope⁴².

Enzyme-Linked Immunosorbent Assay (ELISA)

Brain samples were harvested at day 3 after ICH, and levels of IL-18 and IL-1 β were examined with ELISA Kits (Jiangsu Enzyme Biotechnology, China). In addition, the kinase activity of LRRK2 was determined with ELISA Kit (Jiangsu Enzyme Biotechnology, China).

Co-Immunoprecipitation Assay

To detect whether LRRK2 was combined with NLRC4, the LRRK2-antibody was incubated with magnetic beads to form a complex in solution. Then, the magnetic beads were separated and the antibody was recycled. Next, the tissue sample was incubated with beads which would bind to the antibody to form an antibody/antigen complex, and the tissue sample was dissociated. To pull down the complex from the beads, loading buffer was diluted with PBS and added to the complex with the beads subsequently abandoned. The LRRK2 proteins were separated by SDS-PAGE for western blot analysis using anti-NLRC4 to determine the NLRC4. The same method was used to detect whether NLRC4 was combined with LRRK2, and whether NLRC4 was combined with pro-caspase-1.

Statistical Analysis

Data were described as mean \pm SD. GraphPad Prism software (version 7.0) was employed to conduct the statistical analyses. One-way ANOVA and Tukey's multiple comparisons test were used to analyzed parametric data. $p < 0.05$ indicated significant difference.

3. Results

3.1 The NLRC4 inflammasome was activated following ICH

To investigate whether the NLRC4 inflammasome was activated after ICH, Western blot was used to detect the levels of pNLRC4 and immunoprecipitation was used to detect the combination of NLRC4 with pro-caspase-1. The results indicated increased pNLRC4 levels after ICH, which may reached the peak at about 72 h after intracerebral hemorrhage (Fig.1, A and C). There was no significant difference in NLRC4 levels between the six groups (Fig.1, A and B). The results of Co-Immunoprecipitation showed that NLRC4 and pro-caspase-1 were combined with each other in the rat brain tissue 72 hours after ICH (Fig.1, D). These results revealed activated NLRC4 inflammasomes after ICH.

3.2 NLRC4 knockdown may enhanced neurobehavioral functions, relieved brain edema, decreased neuronal death, and extenuated the damage of the blood-brain barrier following ICH

We subsequently used modified Neurological Severity Scores (mNSS) and brain water content to detect the role of NLRC4 in ICH-induced neurological injury. The results showed that, compared with Sham group, the ICH group at 72 hours demonstrated severe deficits in mNSS and higher brain edema. Following NLRC4 siRNA mixture, significant improvement was seen among the mNSS at 72 h compared to ICH and ICH+NC group (Fig.2, A). The brain edema in the ipsilateral brain and contralateral brain after NLRC4 siRNA injection reduced significantly at 72 h compared to ICH and ICH+NC (Fig.2, B). Correspondingly, compared with the sham group, the HE staining evidenced a disorderly cytoplasmic loose, karyopyknosis and edema of the neurons in the ICH group. This alteration could be significantly reversed after treatment with NLRC4 siRNA (Fig.2, C). Nissl staining showed decreased nissl bodies in the ICH group compared to the Sham samples. The number of the nissl bodies was significantly increased through the treatment of NLRC4 siRNA. (Fig.2, D). NLRC4 siRNA injection decreased the EB leakage from blood vessels into the brain tissue at 72 hours after ICH (Fig.2, E). The autofluorescence intensity of Evans blue was declined

with the treatment of NLRC4 siRNA(Fig.2, F). Altogether, these results showed that NLRC4 may aggravate ICH-induced brain injury among rats.

3.3 Neutrophil infiltration and IL-1 β , IL-18 and cleaved caspase-1 levels after intracerebral hemorrhage were decreased by NLRC4 knockdown

To explore NLRC4's role in ICH-related inflammation, siRNAs were injected to knock down the NLRC4. Western blot revealed that, compared with negative control siRNA (ICH+NC) group and ICH group, pNLRC4, cleaved caspase-1, IL-1 β and IL-18 levels were reduced significantly by NLRC4 siRNA injection (Fig.3, A). Accordingly, ELISA showed that, compared with ICH+NC group and ICH group, the levels of IL-18 and IL-1 β also declined (Fig.3, D and E). To understand the effects of NLRC4 on neutrophil infiltration, we used immunostaining to detect brain tissue myeloperoxidase (MPO) levels 72h following ICH. Immunostaining ($\times 200$ and $\times 400$) results showed that NLRC4 siRNA treatment reduced MPO-positive cells around the hematoma significantly when compared to ICH group and ICH+NC group (Fig.3, B and C). This data suggested that NLRC4 knockdown mitigated the neuroinflammation after ICH.

3.4 LRRK2 kinase activity is involved in the activation of NLRC4 inflammasomes

GNE7915 (LRRK2 inhibitor) was used to detect LRRK2 kinase's role in the neuroinflammation induced by the NLRC4 inflammasome following intracerebral hemorrhage. ELISA results showed that GNE7915 reduced the LRRK2 kinase activity in peri-hematoma area(Fig.4, A) and prevented the phosphorylation of LRRK2 at Ser935(Fig.4, C). But it also reduced the level of LRRK2(Fig.4, C). Immunoprecipitation results revealed that treatments with GNE7915 inhibited the formation of LRRK2–NLRC4 complex (Fig.4, B) and Western blot showed that GNE7915 attenuated caspase-1, IL-1 β and IL-18 induced by the NLRC4 inflammasome activation in peri-hematoma area following ICH (Fig.4, C-E). These results implicated the important role of LRRK2's kinase activity in the activation of NLRC4 inflammasomes following ICH.

3.5 RGS2 reduces the combination of NLRC4 and LRRK2

To detect the effect of RGS2 on combination of NLRC4 and LRRK2 following intracerebral hemorrhage (ICH) in rats. Short hairpin (sh) RNA was designed and cloned into a lentiviral vector (LV) to knock down the expression level of RGS2. Lentivirus containing RGS2 was designed to overexpress RGS2. Immunoprecipitation results revealed that Lentiviral-RGS2 prevented the combination of LRRK2 and NLRC4, conversely, shRNA-RGS2 promoted the combination of LRRK2 and NLRC4(Fig.5, A). Immunofluorescence colocalization results(Fig.5, B and D) were consistent with the results of immunoprecipitation. The Pearson's coefficient and overlap coefficient were lower in ICH+Lentil-RGS2 group than those in ICH and ICH+NC groups (Fig.5, C). Conversely, the Pearson's coefficient and overlap coefficient were higher in ICH+shRGS2 group than those in ICH and ICH+NC groups (Fig.5, C). These results suggested that RGS2 may be able to regulate the combination of LRRK2 and NLRC4 during intracerebral hemorrhage.

3.6 RGS2 restrains the neuroinflammation induced by the NLRC4

To explore RGS2's effects on the neuroinflammation by NLRC4 inflammasome activation, short hairpin (sh) RNA was used to knock down the expression level of RGS2, and siRNAs were injected to knock down the NLRC4. The results of the Western blot showed that shRNA-RGS2 increased the expression of IL-1 β , caspase-1 and IL-18(Fig.6,D-F), and siRNA-NLRC4 reversed the effect of shRNA-RGS2 on improving the levels of IL-1 β , caspase-1 and IL-18(Fig.6, D-F). The results demonstrated that shRNA-RGS2 treatment significantly enhanced the neuroinflammation induced by the NLRC4.

3.7 RGS2 restrains NLRC4 inflammasome activation through regulating LRRK2 Kinase Activity

To confirm RGS2's effects on the NLRC4 inflammasome activation via LRRK2, short hairpin (sh) RNA was designed to knock down the expression level of RGS2, Lentivirus containing RGS2 was designed to overexpress RGS2, and GNE7915 was injected to reduce LRRK2 kinase activity. Lentiviral-RGS2 reduced the LRRK2 kinase activity, conversely, shRNA-RGS2 enhanced the LRRK2 kinase activity(Fig.7, B). The results of the Western blot showed that Lentiviral-RGS2 reduced the expression of pLRRK2 and pNLRC4, as well as the levels of IL-1 β , caspase-1 and IL-18(Fig.7, A, C and D). ShRNA-RGS2 enhanced the expression of pLRRK2 and pNLRC4, as well as the levels of caspase-1, IL-1 β and IL-18(Fig.7, A, C and D), and GNE7915 reversed the effect of shRNA-RGS2 on improving the levels of pLRRK2, pNLRC4, IL-1 β , caspase-1 and IL-18(Fig.7, A, C and D). The results demonstrated that Lentiviral-RGS2 treatment significantly decreased the activation of NLRC4 inflammasome compared with the ICH group, while treatment with shRNA-RGS2 had a contradictory effect. GNE7915 reversed the effect of shRNA-RGS2 on the activation of NLRC4 inflammasome.

4. Discussion

The role of the NLR family in neuroinflammation is well known, especially NLRP1 and NLRP3. However, there are currently few studies on the role of NLRC4 in neuroinflammation. Thus, in this study, we explored the expression of NLRC4 and its role in neuroinflammation induced by ICH. It was found that the NLRC4 inflammasome was activated after ICH and the brain injury induced by ICH was significantly mitigated when NLRC4 was knocked down in rats. Moreover, our data showed that LRRK2 kinase contributed to NLRC4 inflammasome activation, and RGS2 could regulate the activation of the NLRC4 inflammasome by reducing LRRK2 kinase activity in ICH models. These findings indicated that blocking NLRC4 may be a novel potential therapeutic target after ICH.

The pathogenesis of ICH-induced brain injury includes primary brain injury and secondary brain injury (SBI). The primary brain injury is due to the mechanical effect of hematoma and the SBI is caused by its toxic products⁴³. Increasing evidence has shown that SBI is a key factor in the deterioration of the neurological function after ICH⁴⁴. SBI is inflammatory, oxidative, autophagic, and apoptotic^{44, 45}, leading to the destruction of blood-brain barrier and massive neuronal cell death⁴⁶. Increasing evidence has indicated that the inflammation induced by innate immune system plays an important role in SBI after ICH^{47, 48}. The NLR family, intracellular innate immune sensors, are responsible for processing the pro-IL-1 β and pro-IL-18 into maturation state to promote inflammation^{49, 50}. Previous studies have shown

that NLRC4 could be a Pathogen Associated Molecular Pattern(PAMP) sensor in bacterial inflammatory responses^{51, 52}. However, neuroinflammation, a type of sterile inflammation, is activated by recognizing Damage Associated Molecular Pattern(DAMP) sensor¹³. Our data discovered that NLRC4 could be a DAMP sensor in neuroinflammation after ICH. In this study, it was found that NLRC4 reached the peak of phosphorylation at Ser533 on the 3rd day and the NLRC4 inflammasome was activated after ICH, which corresponded to the peak of proinflammatory cytokine IL-1 β at 2-3 days after ICH⁵³. A study in mice has shown that NLRP3 reached the peak at 12 h after ICH⁵⁴. The difference of expressions between NLRC4 and NLRP3 may be attributed to the expression of NLRP3 mainly in microglia⁵⁴ and the expression of NLRC4 mainly in astrocytes⁵⁵. A research on NLRC4^{-/-} mice after ischemic stroke demonstrated that the NLRC4 inflammasome contributes to acute brain injury⁵⁵. Moreover, the NLRC4 inflammasome is reported to promote alcohol-induced liver injury⁵⁶ and breast cancer progression⁵⁷. Similar to these studies, our results showed that NLRC4 knocked down with siRNAs also reduced brain damage by decreasing IL-1 β , IL-18 and caspase-1, hence reducing neutrophil infiltration, neuronal cell death and blood-brain barrier injury. Overall, our results indicated NLRC4 inflammasomes may result in the aggravation of intracerebral hemorrhage-related inflammation.

It was concluded that NLRC4 inflammasomes are involved in intracerebral hemorrhage-induced inflammation. Nevertheless, molecular mechanisms of NLRC4 inflammasome activation in intracerebral hemorrhage elicited brain injury are poorly known. A recent study has pointed out that LRRK2 kinase activity is related to the activation of the NLRC4 inflammasome in response to Typhimurium infection²⁸. LRRK2 kinase activity is considered as the key factor of PD pathogenesis^{58,59, 60}. Cao and colleagues found that LRRK2 was upregulated following ICH, and aggravated SBI induced by ICH in rats^{36, 61}. Based on these evidence, we proposed that LRRK2 promoted neuroinflammation induced by the NLRC4 inflammasome through the phosphorylation of NLRC4. GNE7915, a highly selective, potent, and BBB-penetrable LRRK2 inhibitor⁶², was used to decrease the LRRK2 kinase activity. A report indicated that the activity of LRRK2 kinase can indirectly regulate the phosphorylation of Ser935, and the level of phosphorylation of Ser935 can be used to assess the relative activity of LRRK2 inhibitors⁶³. We found GNE7915 reduced the LRRK2 kinase activity as well as the phosphorylation of LRRK2 at Ser935. Accordingly, IL-1 β , caspase-1, IL-18 and pNLRC4 levels were also decreased by GNE7915 as expected. Many studies are consistent with our results. George T and his colleagues reported that LRRK2 may result in neuronal apoptosis after cerebral ischemia through modulating the phosphorylation of a microtubule-associated protein Tau, which regulates neurite outgrowth and axonal transport⁶⁴. Similarly, reducing LRRK2 levels ameliorated injured brain region(TBI), induced neuronal apoptosis, BBB permeability, brain edema and neurological impairment through a p38/Drosha Signaling Pathway⁶¹. LRRK2 plays a critical role in the regulation of many signaling pathways as a result of its LRRK2 kinase. Therefore, LRRK2 kinase activity may be related to NLRC4 inflammasome activation after ICH.

How is LRRK2 kinase activity regulated in the neuroinflammation induced by ICH ? LRRK2, due to its complex structure, is also a Roco protein. It is an atypical G-protein, which is a member of Ras/GTPase superfamily called the Ras of complex proteins (Roc)⁶⁵. It has been shown that Rab GTPase activity is regulated by GEF, GAP, and GDI proteins⁶⁶. RGS2 has been

reported as a physiological GTPase Activation Protein(GAP) of LRRK2³². RGS2 has been regarded as a controller of GPCR and linked G protein signaling. RGS terminates the signal through speeding the intrinsic activity of GTPase in the G protein, which returns the G protein to the receptor in its GDP-bound form (inactive) ⁶⁷. RGS2 was considered as a key regulator of AHR⁶⁸. This resulted from the specific interaction between RGS2 and G proteins, which was dependent on the linked GPCR's selective recognition ⁶⁹.RGS2 was also reported to play a protective role in airway inflammation through reducing the number of granulocytes (neutrophils and eosinophils) and the release of inflammatory and chemokines⁷⁰. Similarly, we discovered that RGS2 exerted a protective role in the neuroinflammation induced by the NLRC4 inflammasome following ICH by regulating the LRRK2 kinase activity, which may not be related to GTPase activity. There is a controversy about the expression level of RGS2 in brain tissues under pathological conditions. It has been reported that, when exposed to inflammatory factors TNF- α and IL-1 β , the expression of RGS2 was decreased in astrocytes⁷¹. Contrary to this study, RGS2 was reported to be up-regulated in integrated microarray analysis results in IS⁷². However, a study has shown that RGS2 is upregulated in cerebral ischemia and promotes apoptosis⁷³. This result is contrary to our results, probably on account of its OGD model in astrocytes. Thus, RGS2 restrains the NLRC4 inflammasome activation after ICH through regulating LRRK2 Kinase activity.

5. Conclusions

In summary, our study indicated that the NLRC4 inflammasome may play a role in ICH-induced inflammatory activation by increasing the neutrophil infiltration and expression of IL-1 β , caspase-1 and IL-18. Our data showed that LRRK2 kinase activity may trigger NLRC4 inflammasome activation. This research provided novel insights into the NLRC4 inflammasome after intracerebral hemorrhage and suggested RGS2's protective role against neuroinflammation elicited by ICH. It also identified RGS2 and LRRK2 as targets for interfering with neuroinflammation due to the NLRC4 inflammasome in ICH.

6. Abbreviations

AP	Ammonium Persulfate
ASC	Apoptosis-associated speck-like protein containing a CARD
DAMPs	Damage-associated molecular pattern
DAPI	4,6-Diamidino-2-Phenylindole
ddH ₂ O	Double distilled water
DEPC	Diethyl pyrocarbonate
DMSO	Dimethyl sulfoxide
ICH	Intracerebral hemorrhage
ICH	Intracranial hemorrhage
IL-18	Interleukin-18
IL-1 β	Interleukin-1 β
LRRK2	Leucine-rich repeat kinase 2
MPO	myeloperoxidase
NLRC4	The NLR family CARD domain-containing protein 4
PAMPs	Pathogen-associated molecular pattern
PRRs	Pattern recognition receptor

RGS2 Regulator of G protein signaling 2
shRNA short hairpin (sh) RNA
siRNA small interference RNA

7. Declarations

Ethical approval and consent to participate: The surgical procedures and animal usages in this study were approved by Chongqing Medical University (NIH Publication No. 85-23, revised 1996) .

Consent for publication: Not applicable.

Availability of data and material: All data generated and analysed during this study are included in this article.

Competing interests: None of the other authors have any conflicts to declare.

Funding: This work was supported by Chongqing Science and Technology Committee, china (No.cstc2016shmszx0432), Natural Science Foundation of Chongqing, china (cstc2015jcyjBX0144) and the National Natural Science Foundation of China (Nos. 81671158 and 81771261).

Authors' contributions: Hui Gan designed the study, made the surgical operation, western blot, ELISA, data analysis and drafted the article. Li Zhang participated in HE staining, Nissal staining and immunofluorescence. Hui Chen, Han Xiao and Lu Wang participated in surgical operation .Xuan Zhai participated in article modification. Ping Liang and Jing Zhao provided funding and edited the manuscript for this study.All authors read and approved the final manuscript.

Acknowledgements: None.

References:

- 1 Feigin VL, Lawes CM, Bennett DA, *et al.* Stroke epidemiology: a review of population-based studies of incidence, prevalence, and case-fatality in the late 20th century. *Lancet Neurol* 2003;2(1):43-53.
- 2 Feigin VL, Lawes CM, Bennett DA, *et al.* Worldwide stroke incidence and early case fatality reported in 56 population-based studies: a systematic review. *Lancet Neurol* 2009;8(4):355-369.
- 3 X Z, SM T, CH L, *et al.* Neutrophil polarization by IL-27 as a therapeutic target for intracerebral hemorrhage. *Nature communications* 2017;8(1):602.
- 4 MF S, PT O, SH K, *et al.* Apoptosis as a form of cell death in intracerebral hemorrhage.%A Qureshi AI. 2003;52(5):1041-1047; discussion 1047-1048.
- 5 Q Y, G C, research ZJTs. An update on inflammation in the acute phase of intracerebral hemorrhage.%A Chen S. 2015;6(1):4-8.

- 6 E M, R V. Neuroinflammation after intracerebral hemorrhage. *Frontiers in cellular neuroscience* 2014;8(undefined):388.
- 7 Lok J, Zhao S, Leung W, *et al.* Neuregulin-1 effects on endothelial and blood-brain-barrier permeability after experimental injury. *Translational stroke research* 2012;3 Suppl 1:S119-124.
- 8 S A, D C, S S, *et al.* Interleukin 18 in the CNS. *Journal of neuroinflammation* 2010;7(undefined):9.
- 9 MT H, MP K, E L. Innate immune activation in neurodegenerative disease. *Nature reviews Immunology* 2014;14(7):463-477.
- 10 MT H, RM M, E L. Inflammasome signalling in brain function and neurodegenerative disease. *Nature reviews Neuroscience* 2018;19(10):610-621.
- 11 MR dZ, NW P, S Z, *et al.* Inflammasomes. *Cold Spring Harbor perspectives in biology* 2014;6(12):a016287.
- 12 P B, VM D. Inflammasomes: mechanism of assembly, regulation and signalling. *Nature reviews Immunology* 2016;16(7):407-420.
- 13 A P, SE H, GD B. Pattern recognition receptors in antifungal immunity. *Seminars in immunopathology* 2015;37(2):97-106.
- 14 TD K, M L, G N. Intracellular NOD-like receptors in host defense and disease. *Immunity* 2007;27(4):549-559.
- 15 P B, J vM, JW J, *et al.* Differential requirement for Caspase-1 autoproteolysis in pathogen-induced cell death and cytokine processing. *Cell host & microbe* 2010;8(6):471-483.
- 16 N VO, L VW, JC S, *et al.* Flagellin-induced NLRC4 phosphorylation primes the inflammasome for activation by NAIP5. *Matusiak M.* 2015;112(5):1541-1546.
- 17 S M, A I-T, K N, *et al.* Phosphorylation of NLRC4 is critical for inflammasome activation. *Qu Y.* 2012;490(7421):539-542.
- 18 CM A-A, M D, AE C, *et al.* Cytoplasmic flagellin activates caspase-1 and secretion of interleukin 1beta via Ipaf. *Miao EA.* 2006;7(6):569-575.
- 19 K N, DM M, D V, *et al.* Differential activation of the inflammasome by caspase-1 adaptors ASC and Ipaf. *Mariathasan S.* 2004;430(6996):213-218.
- 20 KN C, TL R, DB M. Inflammation and neuroprotection in traumatic brain injury. *JAMA neurology* 2015;72(3):355-362.
- 21 K M, J B, C P, *et al.* Sterile inflammation after permanent distal MCA occlusion in hypertensive rats. *Journal of cerebral blood flow and metabolism : official journal of the International Society of Cerebral Blood Flow and Metabolism* 2014;34(2):307-315.
- 22 J L, QQ H. Roco Proteins and the Parkinson's Disease-Associated LRRK2. *International journal of molecular sciences* 2018;19(12):undefined.
- 23 L T, neurodegeneration YJJM. The role of the LRRK2 gene in Parkinsonism. *Li JQ.* 2014;9(undefined):47.
- 24 S J, EW E, WP G, *et al.* Cloning of the gene containing mutations that cause PARK8-linked Parkinson's disease. *Paisán-Ruíz C.* 2004;44(4):595-600.
- 25 P R-R, M R-L, J M-P, *et al.* The G2019S variant of leucine-rich repeat kinase 2 (LRRK2) alters endolysosomal trafficking by impairing the function of the GTPase RAB8A. *The Journal of biological chemistry* 2019;294(13):4738-4758.

- 26 S R, S B, S K, *et al.* The Parkinson disease-linked LRRK2 protein mutation I2020T stabilizes an active state conformation leading to increased kinase activity. *The Journal of biological chemistry* 2014;289(19):13042-13053.
- 27 K M, D B, F G, *et al.* Parkinson-related LRRK2 mutation R1441C/G/H impairs PKA phosphorylation of LRRK2 and disrupts its interaction with 14-3-3. *Proceedings of the National Academy of Sciences of the United States of America* 2014;111(1):E34-43.
- 28 X L, Y L, J Z, *et al.* LRRK2 promotes the activation of NLRC4 inflammasome during Typhimurium infection. *Journal of Biological Chemistry* 2017;292(10):3051-3066.
- 29 KJ G, KE S, JR H. Roles for Regulator of G Protein Signaling Proteins in Synaptic Signaling and Plasticity. *Molecular pharmacology* 2016;89(2):273-286.
- 30 C H, H W, J R, *et al.* RGS2 genetic variation: association analysis with panic disorder and dimensional as well as intermediate phenotypes of anxiety. *American journal of medical genetics Part B, Neuropsychiatric genetics : the official publication of the International Society of Psychiatric Genetics* 2015;151(3):211-222.
- 31 H C, N N, E I, *et al.* Association of RGS2 gene polymorphisms with suicide and increased RGS2 immunoreactivity in the postmortem brain of suicide victims. *Neuropsychopharmacology : official publication of the American College of Neuropsychopharmacology* 2008;33(7):1537-1544.
- 32 J D, H L, M G, *et al.* A Parkinson's disease gene regulatory network identifies the signaling protein RGS2 as a modulator of LRRK2 activity and neuronal toxicity. *Human molecular genetics* 2014;23(18):4887-4905.
- 33 research SLJTs. Age-related comparisons of evolution of the inflammatory response after intracerebral hemorrhage in rats. *Journal of Neuroinflammation* 2012;3(1):132-146.
- 34 C M, J Z, L Z, *et al.* Effects of NLRP6 in Cerebral Ischemia/Reperfusion (I/R) Injury in Rats. *Journal of molecular neuroscience : MN* 2019;undefined(undefined):undefined.
- 35 Q H, Z L, Y W, *et al.* Resveratrol alleviates cerebral ischemia/reperfusion injury in rats by inhibiting NLRP3 inflammasome activation through Sirt1-dependent autophagy induction. *International immunopharmacology* 2017;50(1):208-215.
- 36 Y Z, J Z, Z Z, *et al.* Leucine-rich repeat kinase 2 aggravates secondary brain injury induced by intracerebral hemorrhage in rats by regulating the P38 MAPK/Drosha pathway. *Journal of Neuroinflammation* 2018;17(1):53-64.
- 37 S W, Y Z, B Y, *et al.* C1q/Tumor Necrosis Factor-Related Protein-3 Attenuates Brain Injury after Intracerebral Hemorrhage via AMPK-Dependent Pathway in Rat. *Frontiers in cellular neuroscience* 2016;10(1):237.
- 38 Q H, Z L, C M, *et al.* Parkin-Dependent Mitophagy is Required for the Inhibition of ATF4 on NLRP3 Inflammasome Activation in Cerebral Ischemia-Reperfusion Injury in Rats. *Cells* 2019;8(8):undefined.
- 39 BF W, ZW C, ZH Z, *et al.* Curcumin attenuates brain edema in mice with intracerebral hemorrhage through inhibition of AQP4 and AQP9 expression. *Acta pharmacologica Sinica* 2015;36(8):939-948.
- 40 Y L, G L, XW S, *et al.* Characterization of Axon Damage, Neurological Deficits, and Histopathology in Two Experimental Models of Intracerebral Hemorrhage. *Frontiers in neuroscience* 2018;12(1):928.

- 41 Y S, Y Y, Y C, *et al.* Lipoxin A4 Methyl Ester Reduces Early Brain Injury by Inhibition of the Nuclear Factor Kappa B (NF- κ B)-Dependent Matrix Metalloproteinase 9 (MMP-9) Pathway in a Rat Model of Intracerebral Hemorrhage. *Medical science monitor : international medical journal of experimental and clinical research* 2019;25(undefined):1838-1847.
- 42 Y C, Y Z, J T, *et al.* Norrin protected blood-brain barrier via frizzled-4/ β -catenin pathway after subarachnoid hemorrhage in rats. *Stroke* 2015;46(2):529-536.
- 43 G X, RF K, JT H. Mechanisms of brain injury after intracerebral haemorrhage. *The Lancet Neurology* 2006;5(1):53-63.
- 44 J A, Stroke ZXJ. Molecular pathophysiology of cerebral hemorrhage: secondary brain injury. 2011;42(6):1781-1786.
- 45 RA F, JC G, AL S, *et al.* Cell death in experimental intracerebral hemorrhage: the "black hole" model of hemorrhagic damage. *Annals of neurology* 2002;51(4):517-524.
- 46 R B, JH B, C D, *et al.* Thrombin and hemin as central factors in the mechanisms of intracerebral hemorrhage-induced secondary brain injury and as potential targets for intervention. *Neurosurgical focus* 2012;32(4):E8.
- 47 J W, S D. Inflammation after intracerebral hemorrhage. *Journal of cerebral blood flow and metabolism : official journal of the International Society of Cerebral Blood Flow and Metabolism* 2007;27(5):894-908.
- 48 Y Z, Y W, J W, *et al.* Inflammation in intracerebral hemorrhage: from mechanisms to clinical translation. *Progress in neurobiology* 2014;115(undefined):25-44.
- 49 M L, VM D. Mechanisms and functions of inflammasomes. *Cell* 2014;157(5):1013-1022.
- 50 M L, VM D. Inflammasomes and their roles in health and disease. *Annual review of cell and developmental biology* 2012;28(undefined):137-161.
- 51 JL P, SM S, M T, *et al.* Identification of Ipaf, a human caspase-1-activating protein related to Apaf-1. *The Journal of biological chemistry* 2001;276(30):28309-28313.
- 52 SB M, AP W, RR H. Identification of a sequence in human toll-like receptor 5 required for the binding of Gram-negative flagellin. *The Journal of biological chemistry* 2003;278(26):23624-23629.
- 53 S H, T M. Intracerebral administration of interleukin-1 β and induction of inflammation, apoptosis, and vasogenic edema. *Journal of neurosurgery* 2000;92(1):108-120.
- 54 S C, Q H, H F, *et al.* NLRP3 inflammasome contributes to inflammation after intracerebral hemorrhage. *Ma Q.* 2014;75(2):209-219.
- 55 G C, N L, SM C, *et al.* AIM2 and NLRC4 inflammasomes contribute with ASC to acute brain injury independently of NLRP3. *Denes A.* 2015;112(13):4050-4055.
- 56 DA D, CW K, Y L, *et al.* Alcohol-induced liver injury is modulated by Nlrp3 and Nlrc4 inflammasomes in mice. *Mediators of inflammation* 2013;2013(undefined):751374.
- 57 R K, L P, N B, *et al.* Obesity-associated NLRC4 inflammasome activation drives breast cancer progression. *Nature communications* 2016;7(undefined):13007.
- 58 DG H, M F, SS OS, *et al.* Phenotype, genotype, and worldwide genetic penetrance of LRRK2-associated Parkinson's disease: a case-control study. *The Lancet Neurology* 2008;7(7):583-590.
- 59 E G, S J, A K, *et al.* Kinase activity is required for the toxic effects of mutant LRRK2/dardarin. *Neurobiology of disease* 2006;23(2):329-341.

- 60 E G. Role of LRRK2 kinase activity in the pathogenesis of Parkinson's disease. *Biochemical Society transactions* 2012;40(5):1058-1062.
- 61 Q R, H N, F G, *et al.* LRRK2 Contributes to Secondary Brain Injury Through a p38/Droscha Signaling Pathway After Traumatic Brain Injury in Rats. *Frontiers in cellular neuroscience* 2018;12(undefined):51.
- 62 AA E, X L, C B-G, *et al.* Discovery of highly potent, selective, and brain-penetrable leucine-rich repeat kinase 2 (LRRK2) small molecule inhibitors. *Journal of medicinal chemistry* 2012;55(22):9416-9433.
- 63 N D, M D, F H, *et al.* Inhibition of LRRK2 kinase activity leads to dephosphorylation of Ser(910)/Ser(935), disruption of 14-3-3 binding and altered cytoplasmic localization. *The Biochemical journal* 2010;430(3):405-413.
- 64 T K, R V. Mechanisms of Parkinson's disease-related proteins in mediating secondary brain damage after cerebral ischemia. *Journal of cerebral blood flow and metabolism : official journal of the International Society of Cerebral Blood Flow and Metabolism* 2017;37(6):1910-1926.
- 65 L B, PJ VH. Roc, a Ras/GTPase domain in complex proteins. *Biochimica et biophysica acta* 2003;1643(null):5-10.
- 66 Stenmark H. Rab GTPases as coordinators of vesicle traffic. *Nat Rev Mol Cell Biol* 2009;10(8):513-525.
- 67 S H, JR H. Cellular regulation of RGS proteins: modulators and integrators of G protein signaling. *Pharmacological reviews* 2002;54(3):527-559.
- 68 H J, Y X, PW A, *et al.* Regulator of G-protein signaling 2 repression exacerbates airway hyper-responsiveness and remodeling in asthma. *American journal of respiratory cell and molecular biology* 2015;53(1):42-49.
- 69 SP H, N W, ME L, *et al.* RGS2/G0S8 is a selective inhibitor of Gqalpha function. *Proceedings of the National Academy of Sciences of the United States of America* 1997;94(26):14389-14393.
- 70 T G, M B, M C, *et al.* Protective Roles for RGS2 in a Mouse Model of House Dust Mite-Induced Airway Inflammation. *PloS one* 2017;12(1):e0170269.
- 71 PJ D, M V, A P, *et al.* Inflammation-associated regulation of RGS in astrocytes and putative implication in neuropathic pain. *Journal of neuroinflammation* 2017;14(1):209.
- 72 Q Z, W C, S C, *et al.* Identification of key genes and upstream regulators in ischemic stroke. *Brain and behavior* 2019;9(7):e01319.
- 73 M E, SD K, WM L, *et al.* Ischemia induces regulator of G protein signaling 2 (RGS2) protein upregulation and enhances apoptosis in astrocytes. *American journal of physiology Cell physiology* 2010;298(3):C611-623.

Fig.1 Expressions of NLRC4 and pNLRC4 after intracerebral hemorrhage, and the activation of the NLRC4 inflammasome. (A-C) NLRC4 and pNLRC4 expressions in the peri-hematoma area of sham and ICH rats were detected by Western blot at 3, 24, 48, 72 hours, and 7 days after surgery, respectively (6 rats for each group after ICH). *P < 0.05, compared with Sham group; #P < 0.05, compared with 72h after ICH. (D) The results of co-immunoprecipitation showed that NLRC4 and pro-caspase-1 bound to each other in brain tissues of rats at 72 h post-ICH.

Fig.2 NLRC4 knockdown reduced neurological function damage and decreased brain edema at 72 h after ICH. (A) Modified Neurological Severity Scores (mNSS) for neurological function, (B) Brain edema in ipsilateral brain and contralateral brain for brain water content, (C) HE staining for the morphology ($\times 400$), (D) Nissl staining for the number of nissl bodies ($\times 400$), (E) Evans blue Dye extravasation and (F) autofluorescence ($\times 200$) for the integrity of blood brain barrier in the Sham, ICH, negative control siRNA (ICH+NC), and NLRC4 siRNA (ICH+NLRC4 siRNA) groups at 72h after ICH (6 rats for each group). The error bars indicated mean \pm SD. #P < 0.05, compared with ICH+NC; *P < 0.05, compared with ICH.

Fig.3 NLRC4 inflammasome components were knocked down by NLRC4 siRNA mixture at 72 h after ICH. (A) Western blot assay to detect NLRC4, pNLRC4, IL-1 β , caspase-1 and IL-18, (D and E) ELISA for the expression of IL-18 and IL-1 β (B and C) Immunostaining for MPO-positive cells at peri-hematoma area in sham, ICH, negative control siRNA, and NLRC4 siRNA mixture groups at 72 h after ICH (rats for each group). The error bars represent mean \pm standard error. *P < 0.05, compared with ICH; #P < 0.05, compared with ICH+NC.

Fig.4 LRRK2 inhibitor GNE7915 extenuated the neuroinflammation induced by the NLRC4 inflammasome after ICH.(A) Enzyme-linked immunosorbent assay(ELISA) for LRRK2's kinase activity, (B) Immunoprecipitation assay for combined NLRC4 and LRRK2, (C) Western blot assay to detect LRRK2, pLRRK2, NLRC4, pNLRC4, caspase-1, IL-18 and IL-1 β (D and E)ELISA for the levels of IL-18 and IL-1 β in peri-hematoma area in sham, ICH, ICH+GNE7915, and ICH+DMSO groups at 72 h after ICH (6 rats for each group). The error bars indicated mean \pm standard error. #P < 0.05, compared with ICH+DMSO; *P < 0.05, compared with ICH.

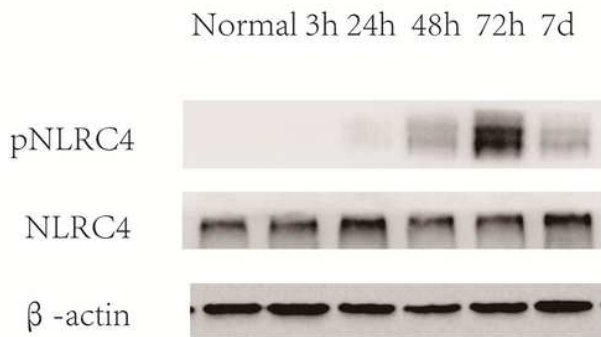
Fig.5 RGS2 affected the combination of NLRC4 and LRRK2 following ICH. (A) Immunoprecipitation assay for the combined NLRC4 and LRRK2, (B and D) Confocal microscopy, and Immunofluorescence colocalized with NLRC4 and LRRK2 for the combination of NLRC4 and LRRK2, and (C) Pearson's coefficient and overlap coefficient for NLRC4 and LRRK2 in peri-hematoma area in ICH, Sham, ICH+shRGS2, ICH+Lentil-RGS2 and negative control lentiviral empty vector(ICH+NC) groups at 72 h after ICH (6 rats for each group). The error bars represent mean \pm standard error. #P < 0.05, compared with ICH+NC; *P < 0.05, compared with ICH.

Fig.6 RGS2 affected the neuroinflammation induced by the NLRC4 following ICH. (A-F) Western blot assay was used to detect the expression of RGS2, NLRC4, IL-1 β , caspase-1 and IL-18 in perihematoma area in ICH, Sham, ICH+shRGS2, ICH+negative control shRNA(ICH+NC shRNA), ICH+shRGS2+si-NLRC4 and ICH+shRGS2+NC siRNA at 72 h after ICH (6 rats for each group). The error bars represent mean \pm standard error.

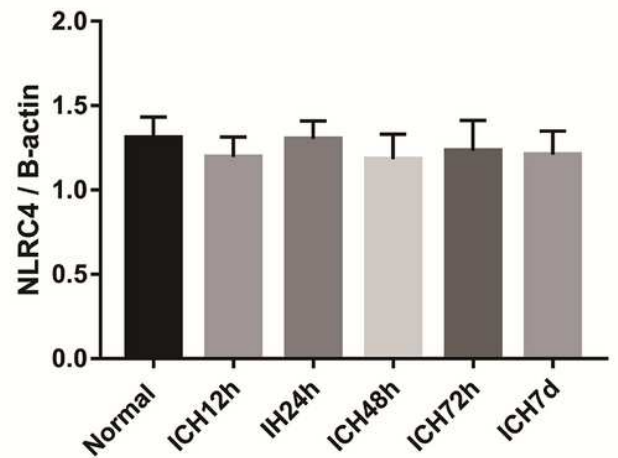
Fig.7 RGS2 affected the neuroinflammation induced by the NLRC4 inflammasome though regulating LRRK2 kinase activity following ICH. (B)ELISA for LRRK2's kinase activity, (A)Western blot assay was used to detect the expression of RGS2, LRRK2, pLRRK2, NLRC4, pNLRC4, IL-1 β , caspase-1 and IL-18, (C and D)ELISA for the levels of IL-1 β and IL-18 in perihematoma area in ICH, Sham, ICH+shRGS2, ICH+Lentil-RGS2, negative control lentiviral empty vector(ICH+NC), ICH+shRGS2+GNE7915 and ICH+shRGS2+DMSO groups at 72 h after ICH (6 rats for each group). The error bars represent mean \pm standard error.

Figures

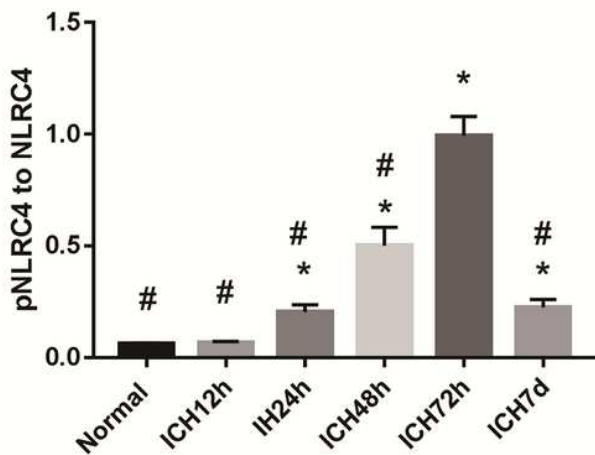
Fig. 1
A



B



C



D

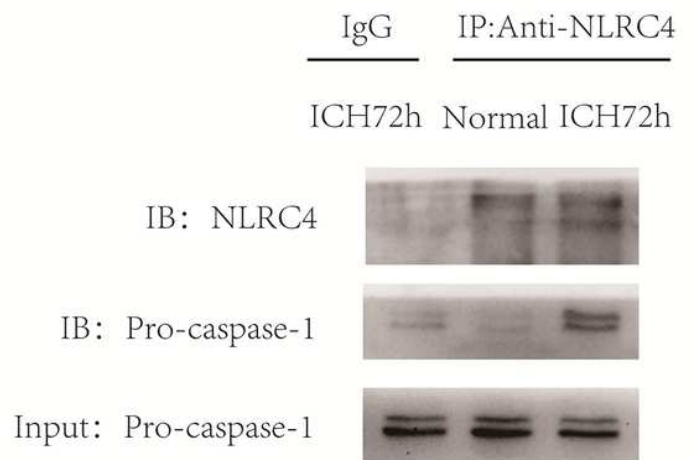


Figure 1

Expressions of NLRC4 and pNLRC4 after intracerebral hemorrhage, and the activation of the NLRC4 inflammasome. (A-C) NLRC4 and pNLRC4 expressions in the peri-hematoma area of sham and ICH rats were detected by Western blot at 3, 24, 48, 72 hours, and 7 days after surgery, respectively (6 rats for each group after ICH). * $P < 0.05$, compared with Sham group; # $P < 0.05$, compared with 72h after ICH. (D) The

results of co-immunoprecipitation showed that NLRC4 and pro-caspase-1 bound to each other in brain tissues of rats at 72 h post-ICH.

Fig. 2

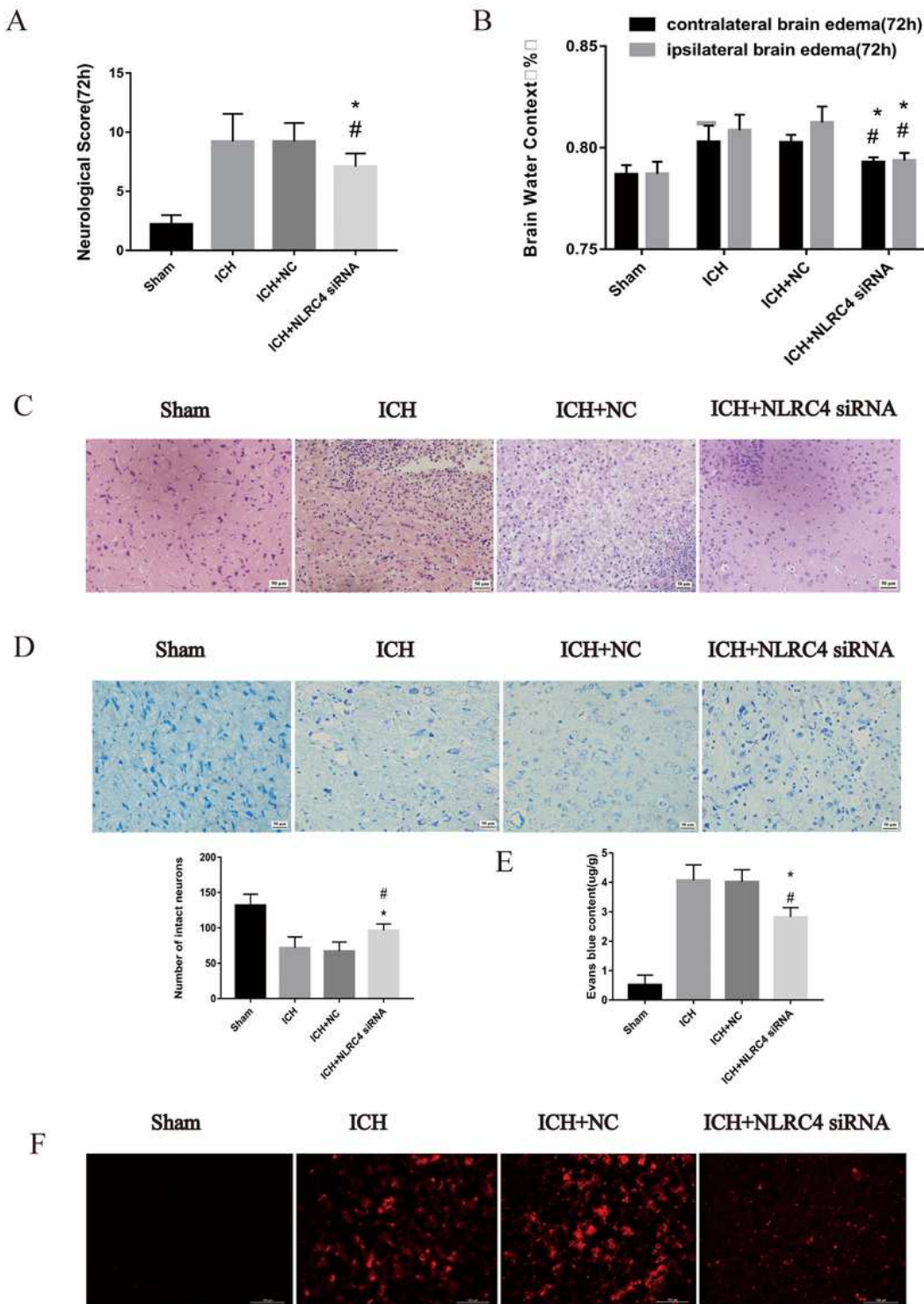


Figure 2

NLRC4 knockdown reduced neurological function damage and decreased brain edema at 72 h after ICH. (A) Modified Neurological Severity Scores (mNSS) for neurological function, (B) Brain edema in ipsilateral brain and contralateral brain for brain water content, (C) HE staining for the morphology ($\times 400$), (D) Nissl

staining for the number of nissl bodies ($\times 400$), (E) Evans blue Dye extravasation and (F) autofluorescence ($\times 200$) for the integrity of blood brain barrier in the Sham, ICH, negative control siRNA (ICH+NC), and NLRC4 siRNA (ICH+NLRC4 siRNA) groups at 72h after ICH (6 rats for each group). The error bars indicated mean \pm SD. # $P < 0.05$, compared with ICH+NC; * $P < 0.05$, compared with ICH.

Fig.3

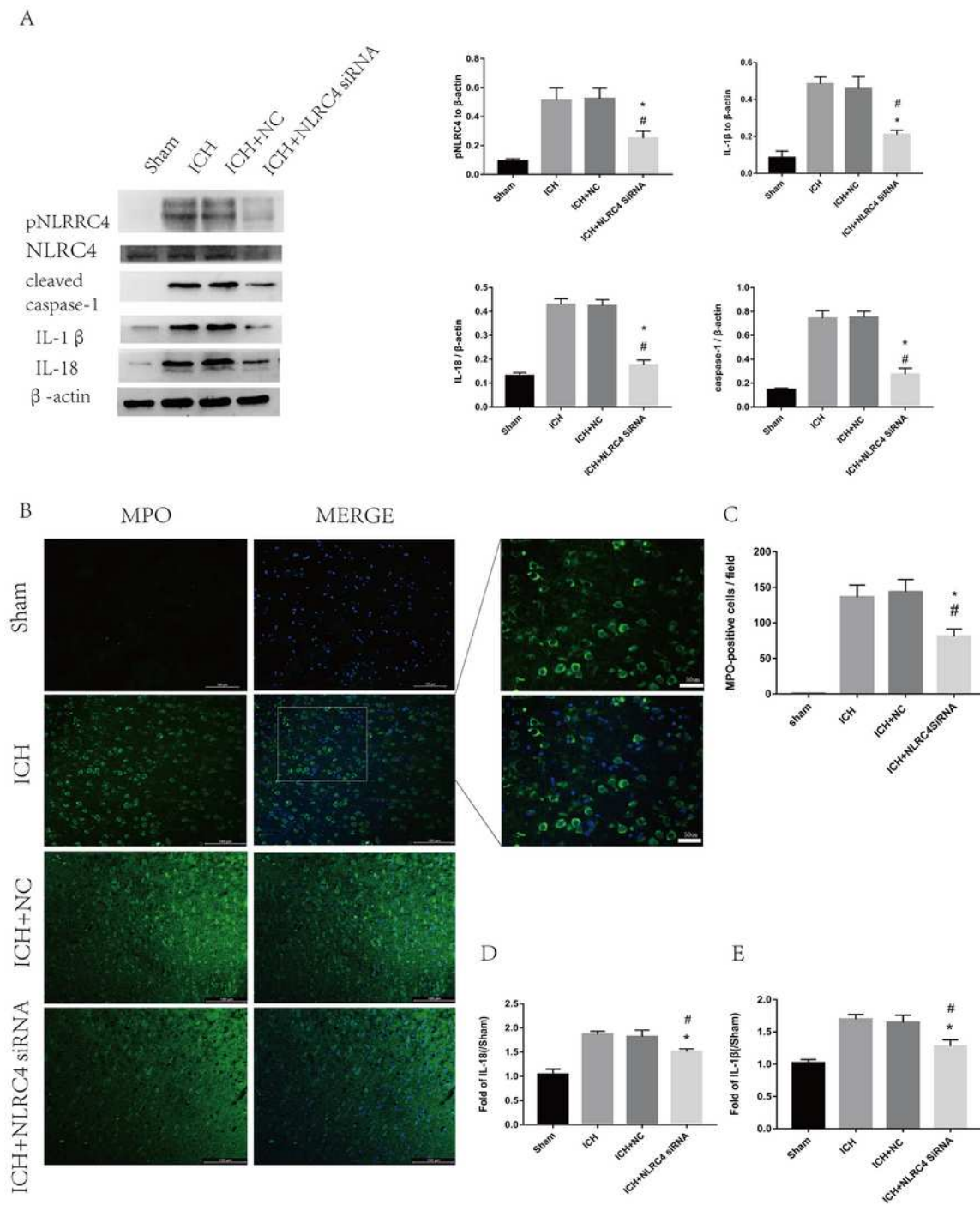


Figure 3

NLRC4 inflammasome components were knocked down by NLRC4 siRNA mixture at 72 h after ICH. (A) Western blot assay to detect NLRC4, pNLRC4, IL-1 β , caspase-1 and IL-18, (D and E) ELISA for the expression of IL-18 and IL-1 β (B and C) Immunostaining for MPO-positive cells at peri-hematoma area in sham, ICH, negative control siRNA, and NLRC4 siRNA mixture groups at 72 h after ICH (rats for each group). The error bars represent mean \pm standard error. * P \leq 0.05, compared with ICH; # P \leq 0.05, compared with ICH+NC.

Fig. 4

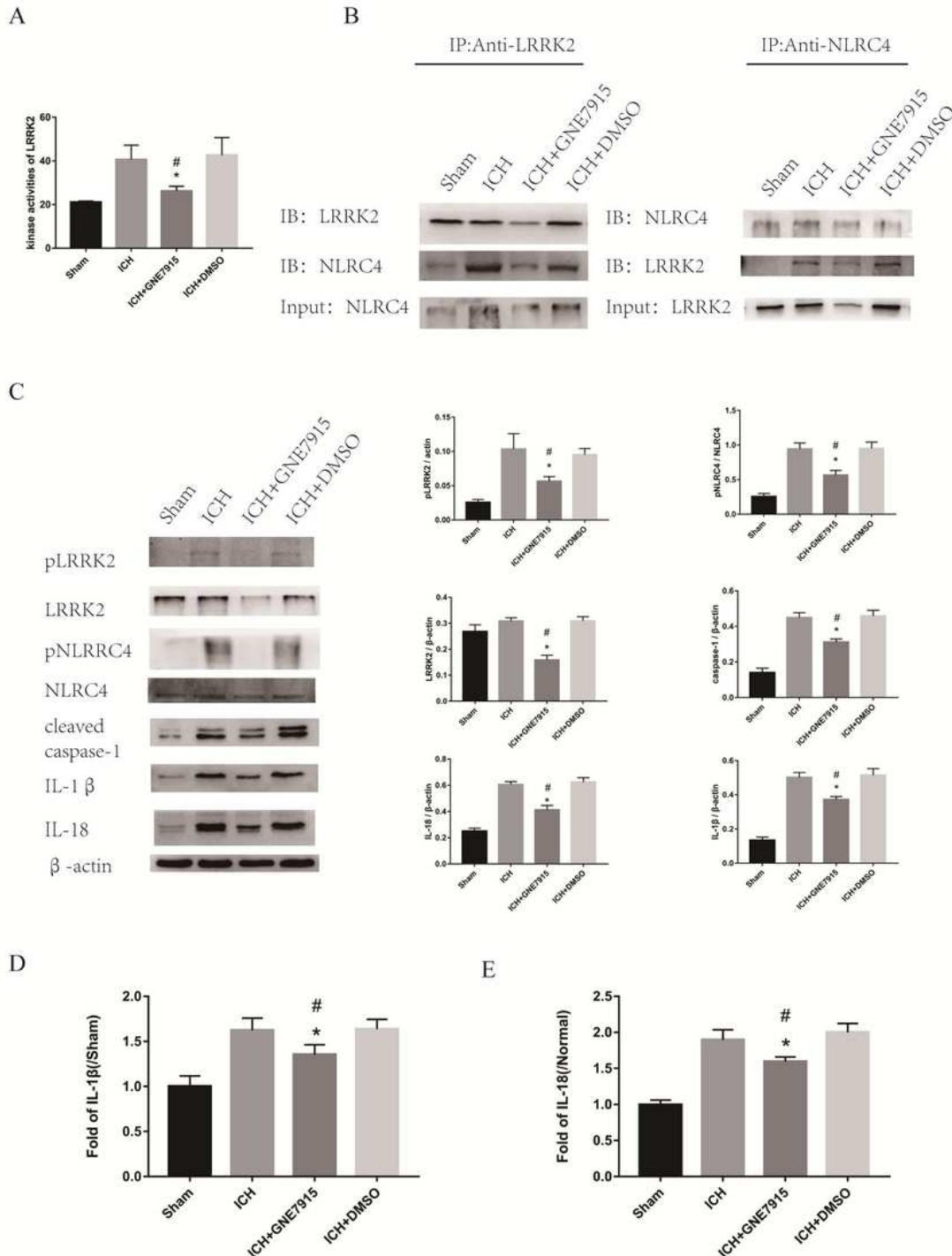
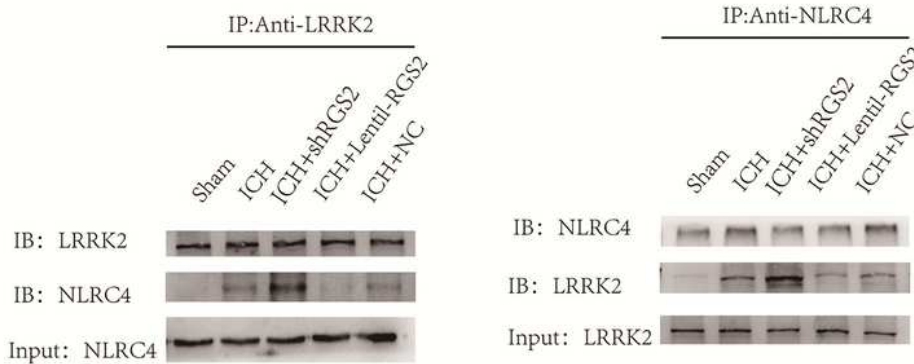


Figure 4

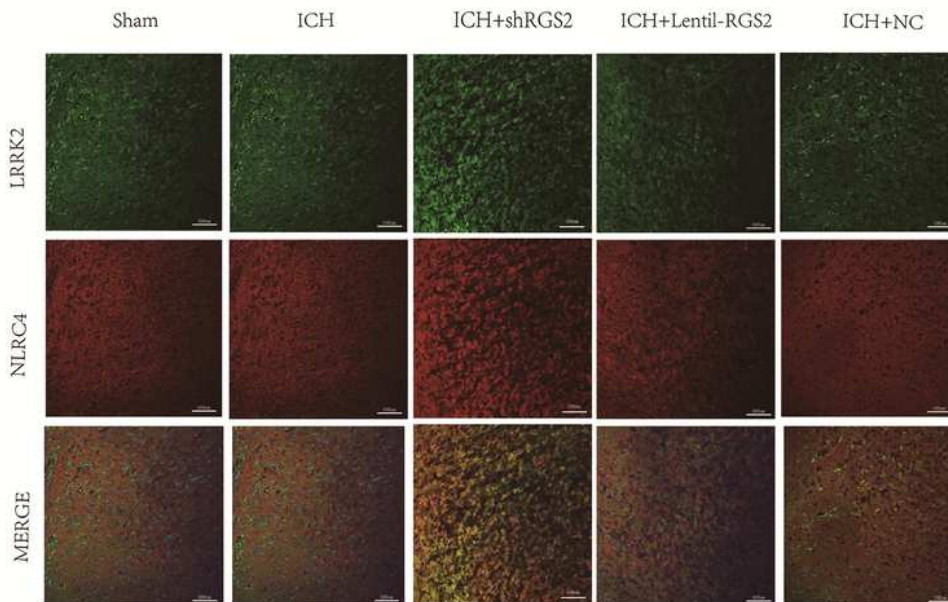
LRRK2 inhibitor GNE7915 attenuated the neuroinflammation induced by the NLRC4 inflammasome after ICH. (A) Enzyme-linked immunosorbent assay (ELISA) for LRRK2's kinase activity, (B) Immunoprecipitation assay for combined NLRC4 and LRRK2, (C) Western blot assay to detect LRRK2, pLRRK2, NLRC4, pNLRC4, caspase-1, IL-18 and IL-1 β (D and E) ELISA for the levels of IL-18 and IL-1 β in peri-hematoma area in sham, ICH, ICH+GNE7915, and ICH+DMSO groups at 72 h after ICH (6 rats for each group). The error bars indicated mean \pm standard error. # $P < 0.05$, compared with ICH+DMSO; * $P < 0.05$, compared with ICH.

Fig.5

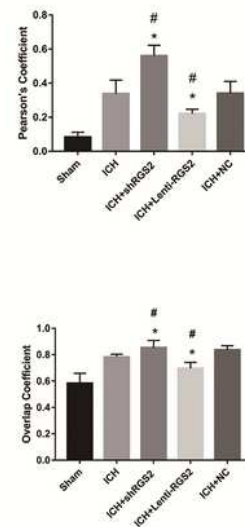
A



B



C



D

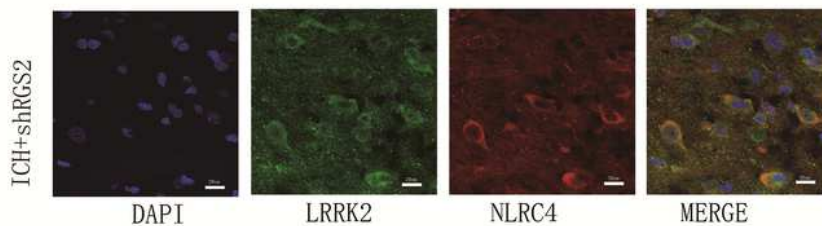


Figure 5

RGS2 affected the combination of NLRC4 and LRRK2 following ICH. (A) Immunoprecipitation assay for the combined NLRC4 and LRRK2, (B and D) Confocal microscopy, and Immunofluorescence colocalized with NLRC4 and LRRK2 for the combination of NLRC4 and LRRK2, and (C) Pearson's coefficient and overlap coefficient for NLRC4 and LRRK2 in peri-hematoma area in ICH, Sham, ICH+shRGS2, ICH+Lentil-RGS2 and negative control lentiviral empty vector(ICH+NC) groups at 72 h after ICH (6 rats for each group). The error bars represent mean±standard error. #P < 0.05, compared with ICH+NC; *P < 0.05, compared with ICH.

Fig.6

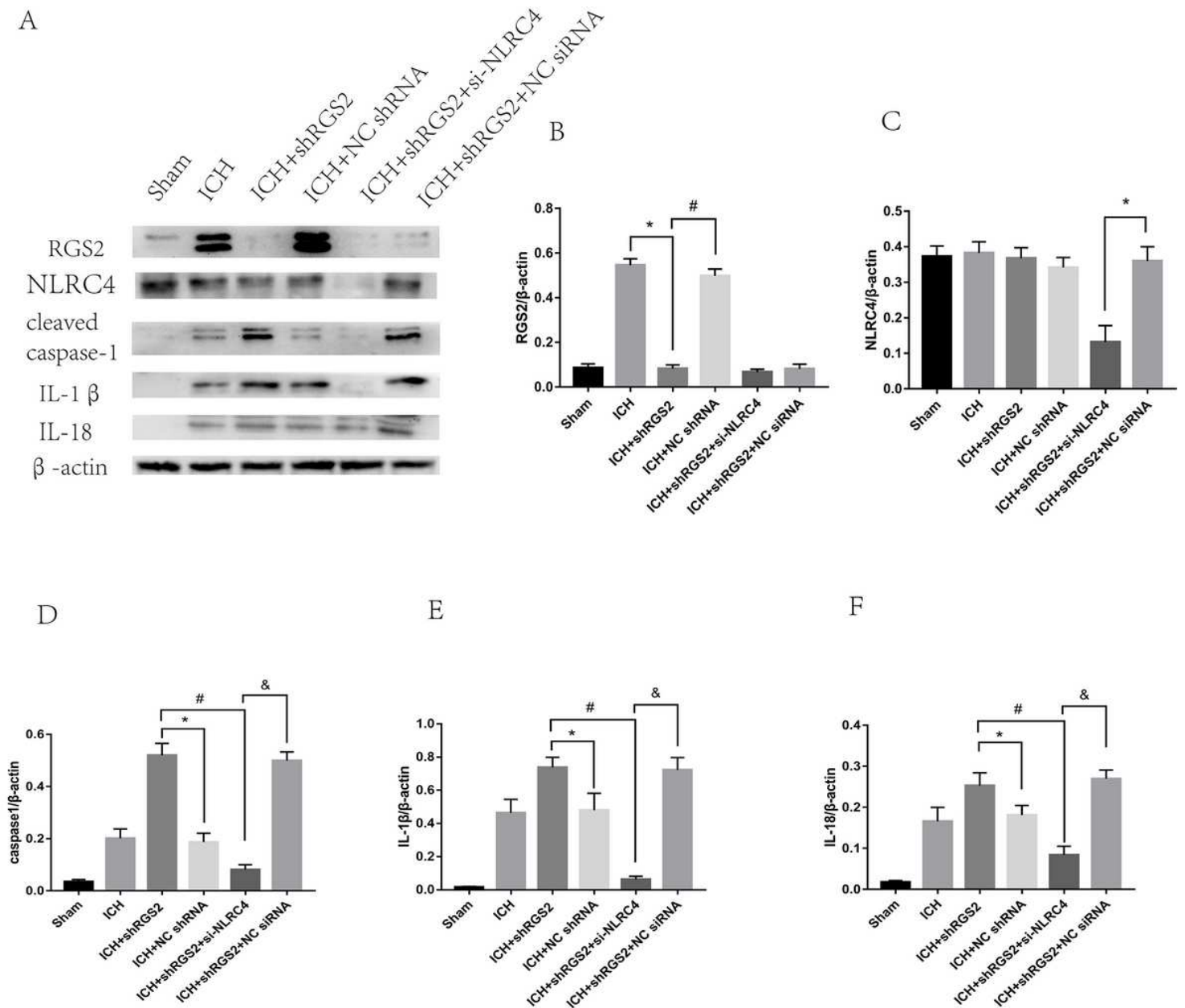


Figure 6

RGS2 affected the neuroinflammation induced by the NLRC4 following ICH. (A-F) Western blot assay was used to detect the expression of RGS2, NLRC4, IL-1 β , caspase-1 and IL-18 in perihematomal area in ICH, Sham, ICH+shRGS2, ICH+negative control shRNA(ICH+NC shRNA), ICH+shRGS2+si-NLRC4 and ICH+shRGS2+NC siRNA at 72 h after ICH (6 rats for each group). The error bars represent mean \pm standard error.

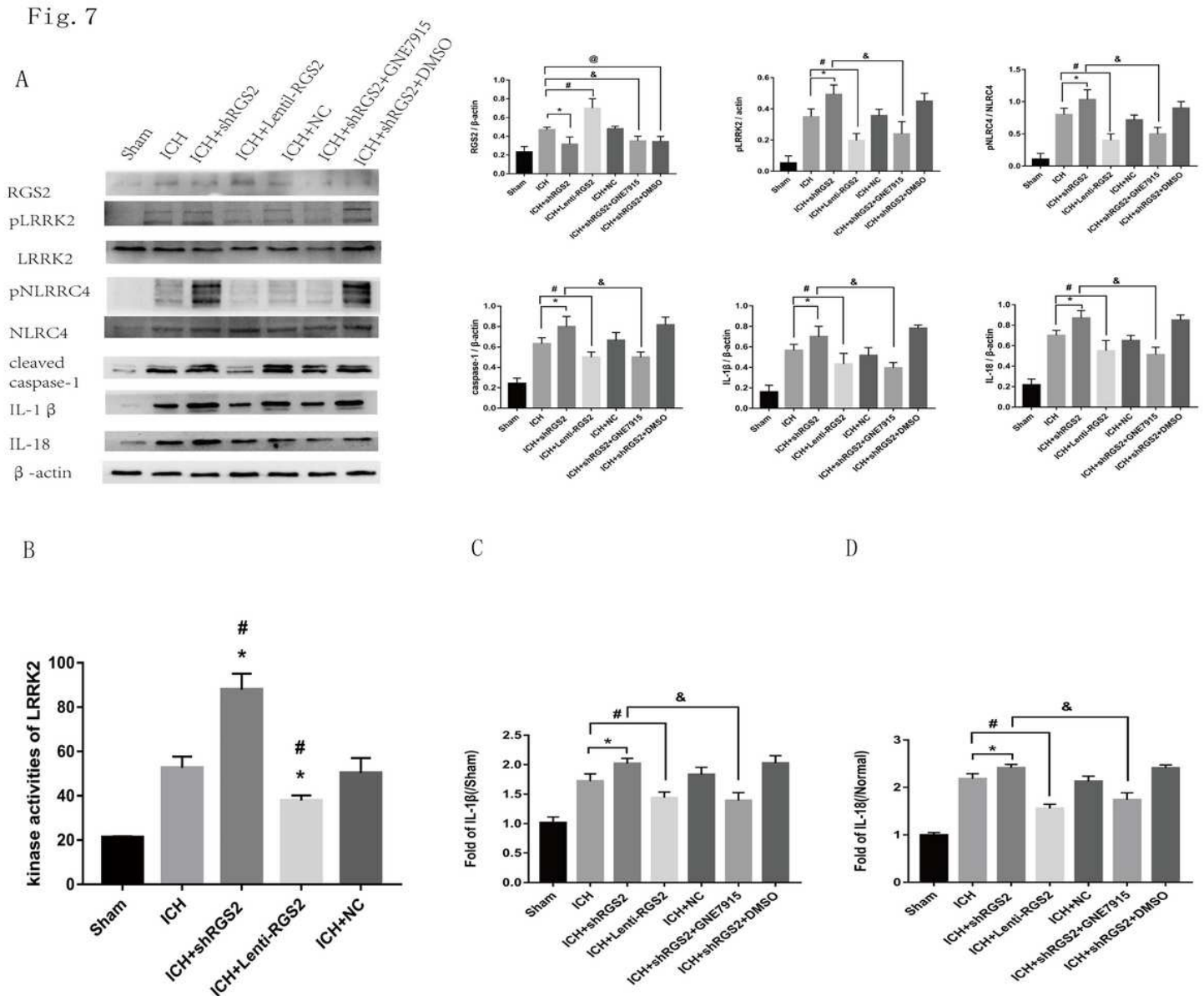


Figure 7

RGS2 affected the neuroinflammation induced by the NLRC4 inflammasome through regulating LRRK2 kinase activity following ICH. (B)ELISA for LRRK2's kinase activity, (A)Western blot assay was used to detect the expression of RGS2, LRRK2, pLRRK2, NLRC4, pNLRC4, IL-1 β , caspase-1 and IL-18, (C and

D)ELISA for the levels of IL-1 β and IL-18 in perihematomal area in ICH, Sham, ICH+shRGS2, ICH+Lentil-RGS2, negative control lentiviral empty vector(ICH+NC), ICH+shRGS2+GNE7915 and CH+shRGS2+DMSO groups at 72 h after ICH (6 rats for each group). The error bars represent mean \pm standard error.